B2

by Rahadi Wirawan

Submission date: 22-Feb-2022 07:01AM (UTC+0700)
Submission ID: 1767877836
File name: Lamp._B2.pdf (416.55K)
Word count: 3446
Character count: 18905

Simulation of Void Detection System using Gamma-Ray Compton Scattering Technique

Mona Berlian Sari[1,*], Rahadi Wirawan[2], Abdul Waris[1], Hong Joo Kim[3] & Mitra Djamal[1,4]

[1]Department of Physics, Faculty of Mathematics and Natural Sciences, Institut Teknologi Bandung, Jalan Ganesha No. 10, Bandung 40132, Indonesia
[2]Physics Study Program, Faculty of Mathematics and Natural Sciences, Universitas Mataram, Jalan Majapahit No. 62, Mataram 83115, Indonesia
[3]Department of Physics, Kyungpook National University, 80 Daehak-ro buk-gu, Daegu 41566, Republic of Korea
[4]Physics Study Program, Faculty of Science, Institut Teknologi Sumatera, Jalan Terusan Jenderal Ryacudu, Way Hui, Jati Agung, Lampung Selatan 35365, Indonesia
*E-mail: berlianona92@gmail.com

Abstract. A simple void detection system for concrete was successfully developed using high-penetration gamma rays with Compton scattering. This research attempted to identify a void in the subsurface of a concrete volume that could not be accessed from any of the sides. Monte Carlo simulation using GEANT4 toolkit was performed to investigate the gamma-ray backscattering events. An NaI(Tl) detector was used with ^{60}Co and ^{137}Cs as gamma-ray sources. The void's location was successfully detected during material target scanning. Density discrepancies conduce variance of the backscattering peak produced due to the presence of a void. Compared to ^{60}Co as the gamma-ray source, ^{137}Cs is a better choice for application in NDT systems using Compton scattering.

Keywords: *backscattering; detector; gamma rays; GEANT4; non-destructive testing.*

1 Introduction

The quality of concrete depends on the stress levels on the surface and in the whole volume. The stress levels are related to the distribution of matter in these areas. A homogeneous distribution of the material inside the concrete's volume is the most important criteria in quality control during the concrete manufacturing process. The effects of bad characteristics such as cracking, defects, etc. increase the probability of building collapse. Besides this, a high elasticity modulus shows the ability of the concrete to carry the load with minimum strain produced. The elasticity modulus depends on the concrete's compressive strength.

Non-destructive testing (NDT) is an excellent measurement method that is usually applied to investigate and analyze material characteristics without

Received November 11th, 2018, Revised Janaury 28th, 2019, Accepted for publication April 10th, 2019.
 ISSN: 2337-5779, DOI: 10.5614/j.eng.technol.sci.2019.51.3.5

causing damage to the material itself. NDT is generally used for mechanical characteristics inspection in quality control of the material produced. Investigation of the material's condition is also necessary for safety reasons. The use of high-precision instruments and excellent products in materials engineering, production, and industrial fields is essential. Many different NDT applications are used in material characteristics measurement using various methods, such as visual testing (Bossi and Giurgiutiu [1]), ultrasonic testing (Darmon, *et al.* [2] and Wu, *et al.* [3]), acoustic emission testing (Holford, *et al.* [4]), electromagnetic testing (Yang, *et al.* [5]), infrared thermographic testing (Angeliki *et al.* [6]), liquid penetrant testing (Kalinichenko, *et al.* [7] and Guirong, *et al.* [8]), optical testing (Liu, *et al.* [9]), digital shearography testing (Hung, *et al.* [10]), eddy current testing (Almeida, *et al.* [11]), and magnetic particles testing (Lu, *et al.* [12]). Most techniques are unable to reach the areas under the inspected surfaces, are suitable only for specific materials, and have high uncertainty. Some of the examination processes have to be repeated to obtain acceptably high precision results. To solve this problem, radiography can be used. Radiography uses X-rays for penetration of the material. One example of an NDT system is using the X-ray backscattering imaging technique for plane materials developed by Kolkoori, *et al.* [13]. Since X-rays have a short transmission distance and performance decreases with increasing distance, high penetration gamma energy should be used.

Gamma rays have high energy and a short wavelength in the electromagnetic spectrum. The energy of the gamma-rays makes inspection of an object under the surface possible. The photoelectric effect, the Compton effects, and pair production are physical phenomena that occur when radiation passes through a material. In NDT applications, gamma-ray penetration is useful for detection of material defects such as voids, inclusions, cracks, inhomogeneous distribution and miss-orientation of fibers. Short wavelength radiation is the best option for investigating thick objects, as described by Gholizadeh [14]. Radioactive sources such as ^{192}Ir, ^{241}Am, ^{60}Co, and ^{137}Cs are commonly used as sources of photon energy in NDT applications.

Several researches on NDT applications using gamma radiation have been conducted, such as observation of the differences in energy distribution and backscattering intensity of 1.12 MeV gamma photons emerging from Zn, Al, Sn, Fe, C as element targets and the compounds as a function of thickness and the atomic number (Z) target by Sabharwal, *et al.* [15]; liquid density identification in polyethylene pipe using a ^{137}Cs gamma ray source by Wirawan, *et al.* [16]; inspection of steel wire ropes on a suspension bridge using a ^{192}Ir gamma-ray source to determine and predict the resistance of steel wire ropes on a suspension bridge caused by corrosion and deformation, as presented by Peng and Wang [17]; and material inspection using gamma scattering techniques with

5 mCi (185 MBq) ^{137}Cs gamma sources and BGO detectors by Chankow, *et al.* [18]. Void inspection in concrete has been performed with various gamma sources, detector types, and simulation methods. An HPGe detector and ^{137}Cs gamma ray source has been used for Portland concrete inspection using MCNP by Priyada, *et al.* [19]; the same kind of gamma source and detector type were used to detect steel embedded in concrete by Margret, *et al.* [20]; and using PENELOPE-2008, gamma-ray exposure in steel and a concrete-lined chamber was calculated by Mer,k *et al.* [21]. Inspection of reinforced concrete using Compton backscattering has been performed using CdTe semiconductor detectors and ^{241}Am gamma sources by Boldo, *et al.* [22].

The focus of this study was the rigorous usage of GEANT4 simulation to investigate a void in a concrete volume and comparison of ^{60}Co with ^{137}Cs gamma source. For these purposes, Monte Carlo simulation was performed. For detector resolution calibration, the simulation data and the experimental data were compared.

2 Method

When gamma rays penetrate a material, Compton scattering is one of the physical processes that may occur. Compton scattering is the interaction of photons and free electrons in the material. When photons and the material collide, some of the energy is transferred to material electrons. In this interaction, a photon with energy E_γ (MeV) is deflected from its original direction with scattering angle θ. Another energy, E_e (MeV), is transferred to the scattered electron or recoil electron. This interaction results in photon scattering and electron scattering. The energy of the scattered photons and the scattered electrons can be seen from Eqs. (1) and (2), respectively [20]. Scattered photons can be detected by a detector.

$$E_{SC} = \frac{E_\gamma}{1+\frac{E_\gamma}{0.511}(1-cos\,\theta)} \quad (1)$$

$$E_e = E_\gamma - E_{SC} \quad (2)$$

Material characteristics such as density and volume have an influence on the scattered photons produced. Beside that, the Compton scattering probability of a material depends on the electron number of the material target and increases linearly to the atomic number (Z) of the material. In the interaction between the gamma rays and the material, the probability of interaction is disclosed in two cross sections, namely the macroscopic cross section, which is expressed as attenuation coefficient μ, and the microscopic cross section. The microscopic

cross section (σ) is expressed as the interaction probability of length and material density.

$$\sigma = \frac{\mu}{N} = \mu \frac{A}{\rho N_A} \tag{3}$$

where N is material density, ρ is absorption material density, A is atomic mass and N_A is Avogadro's number.

Monte Carlo simulation using GEANT4 toolkit was applied in this simulation. Monte Carlo is widely used for the purpose of understanding particle tracking. The GEANT4 (Geometry and Tracking) simulation toolkit was used for constructing the detector system, doing geometry measurements and to predict the experimental result characteristics. An NaI(Tl) scintillation detector was used and the detector response as well as the backscattering peaks were measured. The detector had high detection efficiency and could be operated at room temperature. Another research on the development of an NaI(Tl) detector has been performed by Tam, *et al.* using an Al_2O_3 reflector [23].

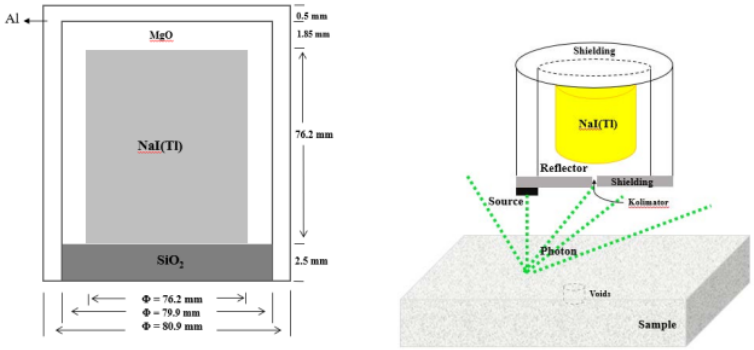

Figure 1 (a) Inner parts configuration of the cylindrical NaI(Tl) scintillation detector [24], (b) measurement design.

Measurements of the response function and NaI(Tl) efficiency showed good agreement with the experimental data. In this study, the detector model was developed using a cylindrical NaI(Tl) with a diameter of 7.62 cm and a thickness of 7.62 cm, covered by aluminum shielding. MgO was used as the reflector and SiO_2 as the absorber. To reduce the background radiation, the inner parts of the detector were surrounded by Pb shielding, as shown in Figure 1(b). This geometry was adapted from Abd-Elzaher, *et al.* [25].

Photon collection is one of the criteria to determine the efficiency and resolution of the detector. Some photons that get into the detector are not directly absorbed by the crystal surface. To recapture these photons, the crystal should be surrounded by a reflector. This reflector needs high reflection coefficients to optimize the light collection. Reflectance may improve photon collection efficiency. A diffuse reflector such as MgO is commonly used to obtain good results. MgO is physically and chemically stable at high temperature. Photon collection is measured by a silicon wafer (SiO_2) photon sensor.

In this simulation, the void was represented by a cylindrical chamber filled with 1.29 mg/cm^3 air density in a volume 60 x 30 x 10 cm^3 ordinary concrete. The detector placement position was varied at 35 measurement points. The measurement process during this simulation aimed to determine the responses of the gamma-ray backscattering energy around 0.2 MeV at various detector positions and also to observe whether concrete density influences the gamma-ray backscattering peak. The full width at half maximum (FWHM) value was determined by using Eq. (4), where σ is the standard deviation, as described by Tam, *et al.* [23], and the detector resolution was determined by using Eq. (5), as described by Kaewkhao, *et al.* [26].

$$FWHM = 2\sqrt{2ln2}\sigma = 2.335\sigma \quad (4)$$

$$Resolution = \frac{FWHM}{E}\,100 \quad (5)$$

3 Results and Discussion

3.1 Resolution and FWHM of the Detector

To determine the detector resolution and the FWHM value, the energy distribution was measured. The experiment was carried out by exposing 1μCi activity of ^{60}Co and ^{137}Cs gamma rays for 10 minutes. A simulation was performed to generate 1x10^8 ^{60}Co events and 5x10^7 ^{137}Cs events with the mentioned activity. The photopeaks from the simulation and the experimental results were compared, as shown in Figure 2.

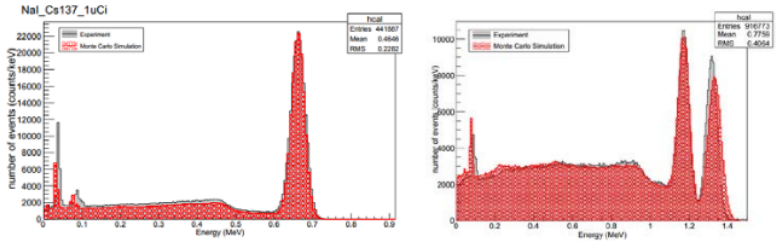

(a) (b)

Figure 2 (a) ^{137}Cs and (b) ^{60}Co energy distribution.

The FWHM of the ^{137}Cs from the experimental results was found to be 0.0433 and the detector resolution calculated was 6.53%. The FWHM and the detector resolution obtained from the simulation results were 0.0441 and 6.66% respectively. These results have good agreement between the experimental data and the simulated data.

For the ^{60}Co gamma source, the FWHM of 1.17 MeV energy from the experiment was 0.0698 and the detector resolution obtained was 5.96%, whereas from the simulation, the FWHM obtained was 0.0752 and the detector resolution was about 6.43%. For ^{60}Co photoelectric energy at 1.33 MeV, the FWHM from the experiment result was 0.0714 and the detector resolution was 5.37%. From the simulation, the FWHM obtained was 0.08 with a detector resolution of 6.04%.

3.2 Void Identification in Concrete

The inhomogeneousness of material density can be examined by investigating the intensity of the scattered radiation [19]. In this simulation, the void was represented by a cylindrical chamber with an air density of about 1.29 gr/cm^3. Because the density of the main concrete was 2.3 gr/cm^3, the intensity of the scattered radiation produced by the main concrete and the void should be different. The simulation was conducted for void detection in a concrete volume of 60 x 30 x 10 cm^3. The measurement setup is shown in Figure 3.

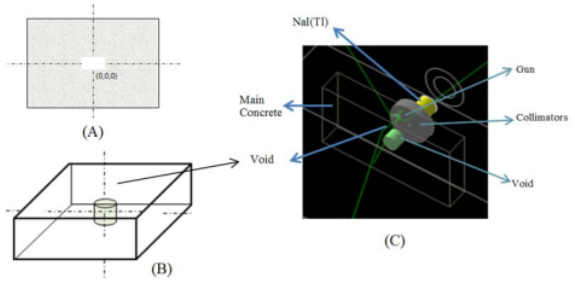

Figure 3 (a) Void position, (b) main concrete and void location, (c) measurement setup in GEANT4.

The void was located at the center of the main concrete and the detector positions for scanning were varied at 35 points. Their 2D plots are shown in Figure 4 in different shades. In Figure 4, the backscattering peaks obtained for each detector position are distinguished by different colors. The backscattering peaks obtained for each point were different from each other according to the number of scattered photons recorded by the detector. When the radiation perceives the concrete as material target and then interacts, the number of photons scattered after this interaction will be detected by the detector as number of counts. This count will increase when the electron density in the material is higher. The count of scattered photons will decrease when the electron density is lower, which indicates the existence of a void. The position of the void is at the (0,0,0) coordinate and is marked with a dark blue color. The void at the center of the concrete, filled with 1.29 gr/cm^3 air, was successfully identified. From Figure 4(a) and (b) it can be seen that ^{137}Cs as the gamma source performed better than ^{60}Co.

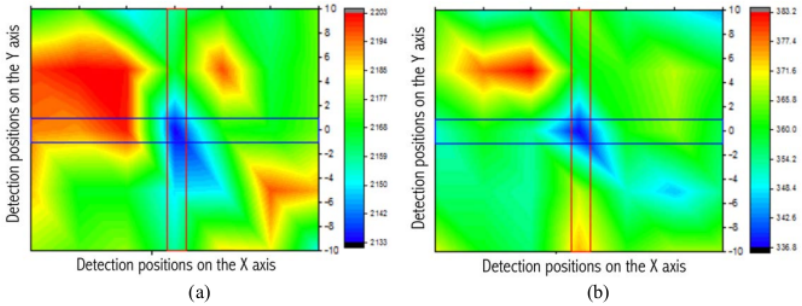

Figure 4 Backscattering peak distribution for void detection at the (0,0,0) coordinate: (a) ^{60}Co, (b) ^{137}Cs.

To see the influence of material density, ordinary concrete was simulated with varying density, i.e. 2.3 gr/cm^3, 2.07 gr/cm^3, 1.61 gr/cm^3, 1.15 gr/cm^3, and 0.69 gr/cm^3 and a cylindrical void. A backscattering peak around the region of interest was found at 0.23 MeV. The number of electrons in a volume element induces backscattering and the density is proportional to the backscattering peak produced, as shown in Figure 5. The R^2 values obtained from exponential fitting for ^{60}Co and ^{137}Cs were 0.97677 and 0.97828, respectively.

The probability of gamma ray interaction with a material is inversely proportional with its density (see Eq. (3)). Increasing the material density will reduce the interaction between photons and the material. As a result, there will be many scattered photons. If a volume element in the material is passed by the photon beam, the reduction of element density conduces photon attenuation and the photon scattering will be reduced (Figure 5). This is similar to the description in Wirawan, *et al.* [24] of the Compton scattering approach in the case of inhomogeneous density. A similar conclusion was also drawn by Priyada, *et al*. [19], namely that the reduction of density by a void causes a subdued backscattering peak. The increase of the Gaussian peak using ^{60}Co as the source is not too significant compared to using ^{137}Cs. This is due to the high energy of ^{60}Co. The decrease of the Gaussian peak in the last point of the ^{137}Cs measurement results was due to the attenuation factor $e^{-\left(\frac{\mu(E_i)}{\rho}\right)\rho r_i}$ in the medium, as described by Wirawan, *et al.* [24].

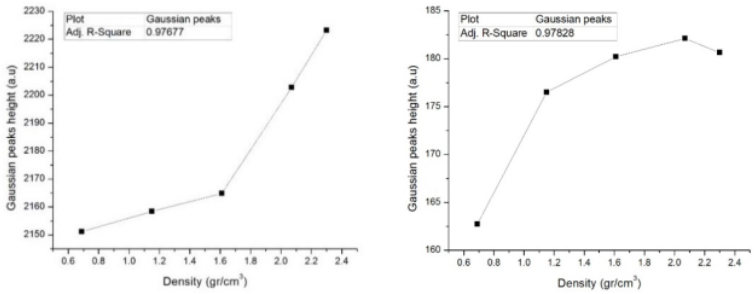

(a) (b)

Figure 5 Correlation of Gaussian peak and concrete density in inhomogeneous density detection: (a) ^{60}Co, (b) ^{137}Cs.

4 Conclusion

Simulation of an NaI(Tl) detector for detecting voids in concrete was successfully performed. The detector and measurement setup were designed using GEANT4 toolkit. The simulation result had good agreement with the experimental data. Detector position placement and void existence influenced the backscattering peaks produced and the position of the void was well identified. Compared to ^{60}Co, ^{137}Cs is more effective as gamma-ray source for application in NDT systems using Compton scattering.

Acknowledgment

This study was supported by a 'Hibah PMDSU' research grant from the Ministry of Research, Technology and Higher Education, Republic of Indonesia.

References

[1] Bossi, R.H. & Giurgiutiu, V., *Nondestructive Testing of Damage in Aerospace Composites*, Polymer Composites in the Aerospace Industry, pp. 413-448, 2015.

[2] Darmon, M., Dorval, V., Djakou, A.K., Fradkin, L. & Chatillon, S., *A System Model for Ultrasonic NDT Based on the Physical Theory of Diffraction (PTD)*, Ultrasonics, **64**, pp. 115-127, 2016.

[3] Wu, B., Huang, Y. & Krishnaswamy, S., *A Bayesian Approach for Sparse Flaw Detection from Noisy Signals for Ultrasonic NDT*, NDT&E International, **85**, pp. 76-85, 2017.

[4] Holford, K.M., Eaton, M.J., Hensman, J.J., Pullin, R., Evans, S.L., Dervilis, N. & Worden, K., *A New Methodology for Automating Acoustic Emission Detection of Metallic Fatigue Fractures in Highly Demanding Aerospace Environments: An Overview*, Progress in Aerospace Sciences, **90**, pp. 1-11, 2017.

[5] Yang, S.H., Kim, K.B., Oh, H.G. & Kang, J.S., *Non-Contact Detection of Impact Damage in CFRP Composites Using Millimeter-Wave Reflection and Considering Carbon Fiber Direction*, NDT & E International, **57**, pp. 45-51, 2013.

[6] Angeliki, K., Fokaides, P.A., Christou, P. & Kalogirou, S.A., *Infrared Thermography (IRT) Applications for Building Diagnostics: A Review*, Applied Energy, **134**, 531-549, 2014.

[7] Kalinichenko, N.P., Kalinichenko, A.N., Lobanova, I.S. & Borisov, S.S., *Methods for the Manufacture of Nonmetallic Reference Specimens for Liquid-Penetrant Inspection*, Russian Journal of Nondestructive Testing, **49**, pp. 668-672, 2014.

[8] Guirong, X., Xuesong, G., Yuliang, Q. & Yan, G., *Analysis and Innovation for Penetrant Testing for Airplane Parts*, Procedia Engineering, **99**, pp. 1438-1442, 2015.
[9] Liu, P., Groves, R.M. & Benedictus, R., *3D Monitoring of Delamination Growth in a Wind Turbine Blade Composite Using Optical Coherence Tomography*, NDT & E International, **64**, pp. 52-58, 2014.
[10] Hung, Y.Y., Yang, L.X. & Huang, Y.H., *Non-Destructive Evaluation (NDE) of Composites: Digital Shearography*, Non Destructive Evaluation (NDE) of Polymer Matrix Composites, pp. 84-115, 2013.
[11] Almeida, G., Gonzalez, J., Rosado, L., Vilaça, L. & Santos, T.G., *Advances in NDT and Materials Characterization by Eddy Currents*, Procedia CIRP, **7**, pp. 359-364, 2013.
[12] Lu, Z.Y., Zhang, Q.L. & Liu, X., *New Magnetic Particle Cassette NDT Intelligent Detection Device*, IEEE, pp. 403-406, 2013.
[13] Kolkoori, S., Wrobel, N. & Zscher, U., *A New X-ray Backscatter Imaging Technique for Non-Destructive Testing of Aerospace Materials*, NDT & E International, **70**, pp. 41-52, 2015.
[14] Gholizadeh, S., *Review of Non-Destructive Testing Methods of Composite Materials*, Procedia Structural Integrity, **1**, 50-57, 2016.
[15] Sabharwal, A.D., Singh, B. & Sandhu, B.S., *Investigation of Multiple Backscattering and Albedos of 1,12 MeV Gamma Photons in Elements and Alloys*, Nuclear Instruments and Methods in Physics Research B, **267**(1), pp. 151-156, 2009.
[16] Wirawan, R., Djamal, M., Waris, A., Handayani, G. & Kim, H.J., *Investigation of Incoherent Gamma-ray Scattering Potential for the Fluid Density Measurement*, Applied Mechanics and Materials, **575**, pp. 549-553, 2014.
[17] Peng, P.C. & Wang, C.Y., *Use of Gamma Rays in the Inspection of Steel Wire Ropes in Suspension Bridges*, NDT & E International, **75**, 80-86, 2015.
[18] Chankow, N. & Pojchanachai, S., *A Unit for Inspection of Materials Using Differential Gamma-Ray Scattering Technique*, Nuclear Instruments and Methods in Physics Research B, **213**, pp. 418-421, 2004.
[19] Priyada, P., Ramar, R. & Shivaramu, *Application of Gamma Ray Scattering Technique for Non-Destructive Evaluation of Voids in Concrete*, Applied Radiation and Isotopes, **74**, pp. 13-22, 2013.
[20] Margret, M., Menaka, M., Venkatraman, B. & Chandrasekaran, S., *Compton Back Scatter Imaging for Mild Steel Rebar Detection and Depth Characterization Embedded in Concrete*, Nuclear Instruments and Methods in Physics Research B, **343**, pp. 77-82, 2015.
[21] Merk, R., Kroger, H., Edelhauser, L. & Hoffman, B., *PENELOPE-2008 Monte Carlo Simulation of Gamma Exposure Induced by ^{60}Co and*

NORM-radionuclides in Closed Geometries, Applied Radiation and Isotopes, **83**, pp. 20-27, 2013.

[22] Boldo E.M. & Appoloni, C.R., *Inspection of Reinforced Concrete Samples by Compton Backscattering Technique*, Radiation Physics and Chemistry, **95**, pp. 392-395, 2015.

[23] Tam, H.D., Yen, N.T.H., Tran, L.B., Chuong, H.D. & Thanh, T.T., *Optimization of the Monte Carlo Simulation Model of NaI(Tl) Detector by GEANT4 Code*, Applied Radiation and Isotopes, **130,** pp.75-79**,** 2017.

[24] Wirawan, R., *Design of NDT System for Material Characterization based on Gamma Ray Scattering using GEANT4 Simulation*, PhD Dissertasion, Department of Physics, Bandung Institute of Technology, 2014.

[25] Abd-Elzaher, M., Badawi, M.S., El-Khatib, A. & Thabet, A.A., *Determination of Full Energy Peak Efficiency of NaI(Tl) Detector Depending on Efficiency Transfer Principle for Conversion from Experimental Values*, World Journal of Nuclear Science and Technology **2**, pp. 65-72, 2012.

[26] Kaewkhao, J., Limkitjaroenporn, P., Chaiphaksa, W. & Kim, H.J., *Non-Proportionality study of CaMoO4 and GAGG:Ce Scintillation Crystals Using Compton Coincidence Technique*, Applied Radiation and Isotopes, **115**, pp. 221-226, 2016.

B2

ORIGINALITY REPORT

8%	8%	8%	9%
SIMILARITY INDEX	INTERNET SOURCES	PUBLICATIONS	STUDENT PAPERS

PRIMARY SOURCES

1	core.ac.uk Internet Source	3%
2	www.onesearch.id Internet Source	2%
3	Submitted to University of Ulster Student Paper	2%
4	Submitted to RMIT University Student Paper	2%

Exclude quotes	Off	Exclude matches	< 2%
Exclude bibliography	Off		